Low power Multi-mode Electrochemical Gas Sensor Array System for Wearable Health and Safety Monitoring

Haitao Li, *Student Member, IEEE*, Xiaoyi Mu, *Member, IEEE*, Yuning Yang, *Student Member, IEEE*, and Andrew J. Mason, *Senior Member, IEEE*

Abstract—**This paper presents an electrochemical gas sensor array system for health and safety monitoring. The system incorporates a custom room temperature ionic-liquid gas sensor array, a custom multi-mode electrochemical sensor readout board, and a commercial low power microcontroller board. Sensors for multiple gas targets were implemented in a miniaturized 2×2 array where each sensor consumes less than 3.2µW and occupies a sensing areavolumeof350mm^3. A novel resource-sharing circuit architecture tailored to the gas sensor array was utilized to significantly decrease power, cost and size. The system supports multiple electrochemical measurement modes to provide orthogonal data to in-module sensor array algorithms for better prediction accuracy. The system achieves a resolution as high as 0.01vol% in amperometry mode and 0.06vol% in AC impedance mode for oxygen as an example target gas.**

Index Terms—**electrochemical gas sensor array; low power**

I. INTRODUCTION

Exposure to air pollution consistently ranks among the leading global causes of illness and mortality [1], and explosive gases are an increasing threat to occupational safety as energy demands rise. Airborne pollutants and explosive gases vary in both time and space. For example, CO and CH_4 can be released from boilers and stoves in homes, and dangerous levels of CH_4 and SO_2 can be found in underground coalmines[2]. To improve scientific understanding of the health impacts of personal exposure to these pollutants and effectively protect workers throughout the vast underground mine environment, individual portable/wearable devices are desperately needed. Such devices should be of small size, low power, low cost, and able to detect multiple gas concentrations in the presence of multiple interferences while permitting easy maintenance.

Existing commercial multiple gas detectors are not suitable for broad individual use due to their high cost, large size and/or large power consumption. In addition, the frequent maintenance required by some of these sensors raises their operating cost and lowers their feasibility. Significant energy has been devoted to the research and development of gas sensing systems. A wireless gas monitoring system has been developed, but it can only monitor one gas[3]. A portable gas detection system has been presented[4], but it can only measure volatile organic compounds. Single-chip gas recognition systems have been reported[5, 6], but these devices cannot measure gas concentrations. As a result, a new portable/wearable system is urgently needed to measure the concentrations of multiple explosive and toxic gases.

To meet this demand, we have developed an intelligent electrochemical gas analysis system (iEGAS) that can measure multiple target gases while providing low power consumption, small volume and easy maintenance. iEGAS consists of room temperature ionic-liquid (RTIL) interfaces embedded in an electrochemical sensor array, a multi-mode electrochemical instrumentation board (MEIB) that enables orthogonal sensing modes, and embedded controller running a sensor array signal processing algorithm to improve selectivity and prediction of multi-gas concentration. Our team has previously reported RTIL-based electrochemical gas sensors that demonstrate high sensitivity and rapid response to methane and oxygen[7-9]. This paper reports our latest system design progress utilizing this new gas sensor technology with a focuses on system architecture and instrumentation electronics design. This paper is a significant extension of our previous conference paper[10], that adds test results of SO_2 sensors, NO_2 sensors, sensor array power consumption, and full instrumentation system characterization, and it includes a comparison to commercial gas sensors. Section II introduces the system architecture and describes the design of the interconnected system layers. Section III outlines the implementation of each layer. In section IV, functionality and performance of the sensor array and instrumentation subsystems are presented to demonstrate the ultra-low power consumption, small volume, and multi-mode operation of the iEGAS gas sensor system.

II. System Design

Simultaneously achieving all of the desired features for a personal gas exposure monitoring system introduces many challenges. To be wearable, the system needs to be miniaturized, light weight, battery powered and either store data, transmit it wirelessly, or both. The system needs to perform measurements intelligently and autonomously, without any external equipment, software, or other support infrastructure. The system must predict mixed gas concentrations accurately and with rapid response while consuming low power for long operation lifetime.

To achieve all these requirements, four design layers were identified for the gas sensing system, namely gas sensors, instrumentation electronics, sensor array processing algorithms and system control. The gas sensor array layer transduces multiple target gas concentrations into electrical signals. The instrumentation electronics layer produces detection-mode dependent stimulus signals and converts gas sensor response signals into a recordable data. The array processing layer executes algorithms designed to identify species and quantify concentrations of target gases within a gas mixture. The system control layer stores system configuration parameters, manages communication, and controls the system to enable autonomous operation. This section analyzes all requirements and constraints from a system-level perspective and shows how they can be mapped to component-level decisions within each design layers.

A. Gas sensor array layer design

1) Gas sensor technologies

A wearable multi-gas sensor microsystem requires gas sensors to be small, low cost, low maintenance, highly sensitive, highly specific, fast response, and low power. The sensor choice must also consider the required measurement techniques and instrumentation electronics, which must adhere to the same requirements as the sensor. The most common gas sensor technologies are metal oxide sensors (MOS),non-dispersive infrared gas sensors(NDIR), catalytic sensors, photoionization detectors (PID), flame ionization detector (FID), thermal conductivity sensor, and electrochemical (EC) sensors[11]. Due to inherent complexity and sophistication, PID, FID and NDIR sensors have high production cost and are difficult to miniaturize. Thermal conductivity sensors can only measure a limited number of gas species, and analytes must possess distinct thermal conductivities from a reference gas. Although catalytic sensors are less sensitive to ambient environment changes and have simple structure, they have very short lifetimes due to poisonings and can only measure combustible gases.

Among gas sensor technologies, both MOS sensors and EC sensors stand out as candidates for wearable systems, especially because their structures are compatible with modern microfabrication processes and are therefore suitable for low cost miniaturization. Table I provides a comparison between these two sensor technologies. Although MOS sensors have extremely long lifetimes and the ability to detect many gases over large concentration ranges, they have poor selectivity

TABLE I
COMPARISON OF GAS SENSOR TECHNOLOGIES THAT ARE MOST SUITABLE FOR SYSTEM MINIATURIZATION

Sensor Type	Advantages	Disadvantages
Metal oxide sensor (MOS)	Long lifetime; low cost; wide range of gases; large detection concentration range; little maintenance; good for miniaturization	Poor selectivity; major dependencies on ambient temperature and humidity; large power consumption; requires oxygen
Electrochemical (EC) sensor:	Ultra-low power consumption; low cost; good selectivity; low detection limit; broad target gases; good for miniaturization	High maintenance if liquid electrolytes are used; interference may happen for some gases; slow response time

because all reducing gases in the atmosphere are detected. Furthermore, MOS sensors consume large power because a heater is needed to maintain an appropriate operating temperature. These disadvantages significantly limit the appeal of MOS sensors for wearable systems. In contrast, EC sensors have ultra-low power consumption, low cost, good selectivity, and can sense a wide range of gases such asCH_4, CO, CO_2, NO, NO_2, SO_2, H_2, and O_2[12-14]. Although traditional EC sensors suffer from slow response time and the high maintenance cost of replacing liquid electrolytes, this paper will demonstrate that these disadvantages can be overcome with a multi-mode EC sensor array using novel materials and structures. Moreover, specificity and interference issues can be overcome using sensor array processing algorithms. Therefore, EC sensors were chosen in our system for multi-gas measurement.

2) Ionic liquid EC gas sensor array

EC gas sensors require the use of an electrolyte, which is an ionically conducting medium that transports charge within electrochemical cells, contacts all electrodes effectively, solubilizes the reactants and products for efficient mass transport, and is chemically and physically stable under all conditions of sensor operation. Traditional electrolytes are classified as liquid electrolytes (aqueous and non-aqueous) and solid electrolytes[15, 16]. Liquid electrolytes have high electrical conductivity but suffer from solvent exhaustion and require periodic electrolyte maintenance. Solid electrolytes overcome this problem but suffer from large power consumption because they must be operated at a high temperature to achieve sufficient ion mobility to sense gases. Room-temperature ionic liquids (RTIL) are novel materials that combine the benefits of both solid and liquid electrolytes. Furthermore, the use of RTILs as electrolytes can eliminate the need for a membrane and thus simplify sensor design. Electrochemical oxidation of NH_3, NO_2 and SO_2 and the electrochemical reduction of O_2 have been reported using RTIL gas sensors, and some have shown wide detection limits, high sensitivity and excellent reproducibility[17, 18]. In addition, RTILs are thermally stable to up to 200°C, enabling them to be employed in harsh, high-temperature environments.

A gas sensor's selectivity is important in a multi-gas measurement system. For EC sensors, selectivity is largely based on the working electrode potential, which depends on the electrolyte and working electrode material. Experiments have

shown that by optimizing the combination of sensor operating potential, electrolytic medium (e.g. RTILs), and working electrode material, a highly selective transducer interfaces can be achieved for mixed gas monitoring[7-9]. Defining a gas sensor's selectivity coefficient as the ratio of the sensor's sensitivity to interfering species and its sensitivity to target gas species, our previous work shows that, by using the RTIL $[C_4mpy][NTf_2]$ as the electrolyte and applying a suitable DC bias, the selectivity coefficient of an O_2 sensor over NO, CO_2, NO_2 and SO_2 is below 0.16%,and the selectivity coefficient over water is 5.8%[9]. These interferences can be further minimized using sensor array processing algorithms.

The main obstacle to response time in RTIL-based EC gas sensors is the slow diffusion of target gases from the RTIL surface to the electrodes[9, 19, 20]. To solve this problem, we introduced a planar-electrode-on-permeable-membrane (PEoPM) structure that avoids the slow diffusion of gas through the RTIL[8]. As illustrated in Fig. 1, the electrodes are fabricated directly on a porous membrane, allowing gas to quickly reach the electrode/RTIL interface. Test results show that the response time of CH_4 can be reduced from 98s to 8s, by 91%, compared to a traditional EC sensor structure [7].

In addition, our previous work has demonstrated that PEoPM EC CH_4 sensors have good selectivity, and reproducibility. It was shown that the maximum interference to CH_4 sensor is below 0.42% (from O_2, H_2, CO_2, NO_2, NO, and SO_2 at maximum concentrations), normalized to 5% CH_4[7]. To demonstrate repeatability of electrochemical impedance spectroscopy mode, measurements of the CH_4 sensor were taken over 90 days and the output capacitance was observed to change by less than 0.3%[7]. Furthermore, an analysis of the DC bias effect on stability of the IL EC sensor can be found in [9]. The short-term stability of our PEoPM sensor for O_2 in chronoamperometry mode was reported in [8] with a standard deviation of only 0.2% over 5000 seconds.

Among the many potential EC measurement techniques, two modes are highly useful for RTIL-based gas sensors. Amperometric mode measures the current generated by reaction of analyte at an electrode at a fixed or variable potential. Electrochemical impedance spectroscopy (EIS) mode measures impedance changes in the double-layer capacitance and the charge-transfer conductance. These two modes could provide orthogonal information to sensor array processing algorithm for better prediction accuracy. Table II summarizes how the characteristics of the sensor array affect the desired system performance goals.
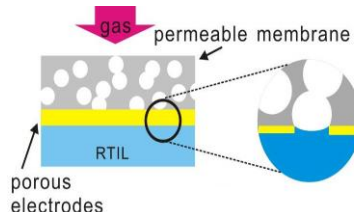

Fig. 1Planar-electrode-on-permeable-membrane structure: response time is improved due to fast gas diffusion through the permeable membrane.
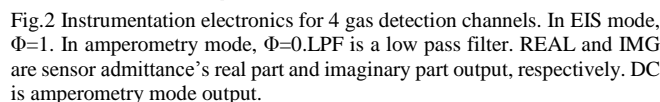
TABLE II
DESIRED SENSOR PERFORMANCE AND SENSOR ARRAY CHARACTERISTICS

System Performance	Relevant Sensor Characteristics
Sensitive	IL EC gas sensors are very sensitive to gas analytes at ppb or ppm level detection limits.
Selective	Specific DC bias voltages on EC sensors maximize selectivity. Dual amperometric and EIS operation modes provide orthogonal information to enhance selectivity through array processing algorithms.
Rapid response	Novel PEoPM structure permits rapid measurement.
Long life time and low maintenance	ILs are chemically and thermally stable in normal atmosphere, thereby enabling long lifetime with minimal maintenance.
High reliability	Amperometric and EIS mode crossly verify each other.
Low cost	EC sensors can be miniaturized using low-cost batch-fabrication microsystem technologies. RTIL is cheap. Low maintenance decreases cost.
Low power	EC sensors consume ultra-low power and can be measured using low power instrumentation Absorption based detection and microelectrodes further reduce EC sensor power consumption.

B. Sensor Instrumentation ElectronicsLayer Design

To support the goals of a portable/wearable system, the instrumentation electronics should have low power consumption, small size and low cost. High-resolution instrumentation electronics are needed to maximize detect limits. The instrumentation electronics should provide stimulation signals to EC gas sensor array and extract sensor output information in two EC modes. A three-electrode EC cell potentiostat should be utilized to maximize the DC bias accuracy on each gas sensor. Our experiments have shown that RTIL-based EC sensor requires a long settling time to stabilize the electrode/RTIL interface after the DC bias is applied or changed. Thus, to create an array of sensors tailored to specific gas targets, each element of the array should be biased to a different target-specific voltage and held at that potential constantly.

Small component count helps to decrease the system power consumption, size and cost. Sharing circuit components between the two EC modes and among gas sensing channels helps to decrease instrumentation electronic component count. A novel resource-sharing instrumentation architecture was developed to share hardware components not only among all the gas sensor array elements but also between different EC detection modes. Four gas sensing channels were designed to demonstrate this technique. All of the EC sensor elements share one signal generator (SigGen) that provides a detection-mode dependent stimulus. Current-to-voltage (I/V) convertors and low pass filters (LPFs) are shared between amperometry mode and EIS mode and controlled by the switch signal Φ. Potentiostats are needed to maintain specific DC bias voltages on the EC sensor array to maximize its gas sensitivity and selectivity. They also apply stimulation signals on the sensor for different operation modes. To minimize interference between the different sensor array elements, four independent

Fig.2 Instrumentation electronics for 4 gas detection channels. In EIS mode, Φ=1. In amperometry mode, Φ=0.LPF is a low pass filter. REAL and IMG are sensor admittance's real part and imaginary part output, respectively. DC is amperometry mode output.

Table III. Components count of instrumentation electronics

	SigGen	gain stage	90° delay	mixer	LPF	I/V	Total count
a	N	2N	N	2N	3N	N	10N
b	1	1	1	2N	2N	N	5N+3

N: total number of gas detection channels.
a: without resource-sharing.; b: with resource-sharing.

potentiostats are provided to control the bias voltage at four independent reference electrodes (RE). Similarly, four independent DC bias voltages, Vdc, are applied to four separate working electrodes (WEs) to establish independent WE-to-RE biasing potentials. The potentiostats are kept on to maintain constant sensor bias voltages. The resulting circuit architecture for four gas detection channels is illustrated in Fig. 2.

In EIS mode, Φ is 1 and all switches except S3 are closed. SigGen generates a 1Hz, 20mV$_{pp}$ sine wave signal to stimulate the gas sensors. This stimulus signal is amplified by A and then provided as input to mixers M1 and M2 to produce reference signals for the lock-in technique. Two LPFs are used to extract the real (REAL) and imaginary (IMG) portions of the gas sensor's complex

Individual gas sensors respond with highest sensitivity to specific portions of the overall complex admittance. For example, in section IV we will use impedance magnitude |Z| for O_2 and NO_2 and real portion of complex capacitance C_{re} for CH_4 and SO_2 to report the highest sensitivity response of these sensors. Both |Z| and C_{re} can be readily converted from REAL and IMG outputs of the MEIB by [1]

$$|Z| = \frac{1}{\sqrt{REAL^2 + IMG^2}} \qquad (1)$$

$$C_{re} = \frac{IMG}{\omega} \qquad (2)$$

where ω is the angular frequency.

In amperometry mode, Φ is 0 and all switches except S3 are open. SigGen provides a fixed DC voltage. Mixer M1 functions as a second gain stage to provide a gain of A for the measured electrode voltage. Out-of-band noise is removed by an LPF to

improve readout resolution.

Although several switches are used in this resource-sharing circuit, they are low cost, take very small area and consume almost no power. Furthermore, the switch control signal Φ can readily be generated by the system control layer. Table III shows that the resource-sharing instrumentation architecture reduces total components count from 10N to (5N+3) for N gas detection channels. As a result, power, cost and size are significantly improved.

Potentiostats provide stimulation signals to the EC sensors. DC bias potentials between WEs and REs of gas sensing channels range from -2V to 2V. To cover this range, a 5V supply and a rail-to-rail amplifier should be used in potentiostats. Circuit stability is also important for EC sensor instrumentation design. An instrumentation structure similar to [21] was used to reject possible oscillations.

C. System Control and Sensor Array ProcessingLayer Design

An autonomous wearable gas sensing system requires an embedded microcontroller (μC). This μC should be power efficient to extend system lifetime. In addition, a μC with built-in analog-to-digital convertor (ADC) is preferred to minimize component count and thus system cost and size. The μC should receive commands from a graphic user interface (GUI) on a PC or smartphone, wirelessly or through a USB port. The μC should also control system operation modes, process sensor array data, generate alerts and send data back to the GUI.

A sensor array processing algorithm runs on the μC to convert MEIB outputs to high sensitivity sensor response parameters. The embedded algorithms also enable identification and quantification of individual gas concentrations within a mixed-gas environment using sensors with imperfect selectivity. In a mixed gas environment, interferences to individual gases combine [22] to amplify the need for removing secondary sensitivities. Current methods implemented in hardware only allow detection of a single gas instead of gas mixtures[23]. Thus, our goal is to enable identification and quantification of individual gas concentrations presented simultaneously in a gas mixture.

A sensor's output can be considered as a function of concentrations of target gases:

$$R = f(C_1, \dots C_i, \dots C_M) \qquad (3)$$

where R is the response of a gas senor and C_i is the concentration of the ith target gas. M is the total number of target gases. To predict a concentration vector C directly from the readout circuits of gas sensors, a regression model can be created such that

$$C = g(R_1, \dots R_j, \dots R_N) \qquad (4)$$

where N is the total number of gas sensors.

We recently reported an analysis of different models including least square (LS), regression tree (RT) and linear model tree (LMT) versus prediction accuracy and running time (or power consumption) in a µC[24]. Synthetic datasets were generated for analysis using a software tool that supports the design of synthetic experiments in machine olfaction[25].The software emulates a virtual sensor array based on a reference dataset recorded from a real gas sensor array measuring three analytes at different concentration levels for ten months. The procedure for analyzing different regression models is shown in Fig. 3. Training samples were first fed into different algorithms to generate regression models. Different parameter settings were chosen to study their effects on the accuracy of regression models. Once a regression model was obtained, testing samples were then input to calculate the prediction error defined by the difference between the estimated and true concentrations normalized by the true concentration.

Table IV list the results of error and running time of different regression models based on a virtual array of four sensors. The study shows that a regression tree is preferable if power consumption is the main consideration over prediction accuracy, while a linear model tree is preferred for high prediction performance with higher power consumption[24].

III. SYSTEM IMPLEMENTATION

EC sensor elements in a PEoPM sensor array were fabricated following reported procedures[26]. To separate the electrochemical elements, O-rings were used to confine the RTIL within individual sensor regions. The O-rings and PEoPM sheets were tightly clamped between two rigid boards containing a hole for gas to enter the electrochemical cell. Printed circuit boards (PCB) were used for the lid and substrate because they are mechanically rigid and facilitate wire routing. A200µm-thick sensing layer of RTIL $[C_4mpy][NTf_2]$ was dropped into the O-ring reservoir of each sensor on the "front" side of the array, as shown in Fig. 4. The resulting 2×2 PEoPM sensor array occupies 1.5" × 1.25" including a connector for interfacing with the MEIB.

The MEIB was constructed using low-power commercial analog electronics in surface mount packages to minimize power and size. Commercial low-power temperature sensor (AD22103) and humidity sensor (HIH5030) were included on the MEIB to monitor the ambient environment and permit compensation of secondary sensitivities of the gas sensor. An ultra-low-power MSP430 Launchpad (Texas Instruments) µC
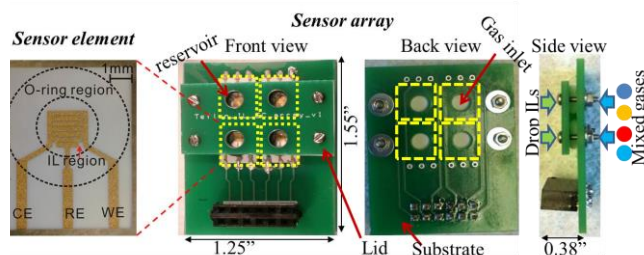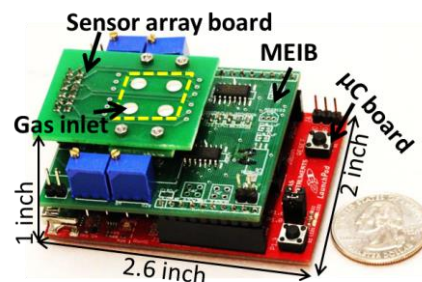

Fig. 5: A prototype iEGAS system with a 4-element RTIL electrochemical sensor array, an MEIB for electrochemical voltage bias and sensor readout, and a µC board for system control and signal processing algorithms to predict multi-gas concentrations.

board was utilized to control system operation, perform environmental compensation, and execute gas sensor array processing algorithms. The µC has eight built-in ADC channels to support all sensor inputs without additional ADC hardware on the MEIB. The user-controlled system operation parameters include sensor scan rate, output storage rate, and output reporting rate. A prototype iEGAS integrating these components was implemented to demonstrate a small and light-weight device for personal safety monitoring, as shown in Fig. 5.The plug-in sensor head can be easily replaced and serviced, thereby decreasing maintenance cost.

IV. RESULTS

To characterize the PEoPM sensor array, it was placed within a multi-gas flow control chamber and connected to a VersaSTAT(Princeton Applied Research) EC instrument. EIS measurements were performed for four example gases of interest to human health and safety protection, CH_4 (methane), O_2, SO_2, and NO_2. The stimulation signal was set to 10mV amplitude at 1Hz. Individual sensors were biased at different DC voltages across WEs and REs to achieve the best specificities. The DC bias voltage values are -0.3V, -0.5V, -1.2V and 1.2V, respectively for the target gases listed above. CH_4 concentration was varied from 0 to 5%; SO_2 concentration was varied from 0 to 25ppm; NO_2 concentration was varied from 0 to 25ppm; O_2 concentration was varied from 10% to 20%. O_2 and NO_2 sensor characterization showed greatest
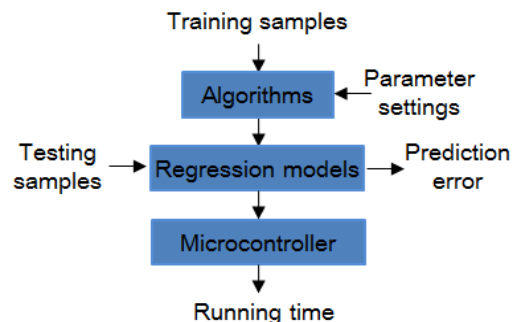

Fig. 3 Procedure for developing regression models and evaluating prediction errors and running time.

Fig 4. Miniaturized 2×2 array of PEoPM sensors. Interdigitated electrodes for EC sensors are shown in the sensor element view on the left side. Four sensor elements were assembled into a sensor adaptor PCB to form a sensor array. Ambient air is sampled through the gas sensor inlet.

Table IV. Error and running time of different regression models on µC.

	LS	RT	LMT
Error	0.24	0.22	0.15
Time (ms)	0.4	1.825	6.2

sensitivity in the impedance magnitude |Z| parameter defined in (1). However, CH_4 and SO_2 demonstrated greater sensitivity within the real portion of complex capacitance C_{re} defined in (2). CH_4 detection is based on an adsorption principle at a specific DC bias. We found that at our stimulation frequency (1Hz), CH_4 sensor has a predominantly capacitive response, and we observed that the impedance phase angle is close to -90° confirming the IL-Au electrode interface behaves like a pure capacitor [7]. At -90° phase angle, the real part of complex capacitance defines the capacitance of the system [27]. The same reason applies to SO_2 sensing. Therefore, C_{re} was used to measure CH_4 and SO_2 concentration. C_{re} is equal to IMG/ω defined in ref. [27]. This argument applies to SO_2 sensing as well, thus CH_4 and SO_2 responses are reported in terms of C_{re}. The resulting calibration curves are shown in Fig. 6. The sensors exhibit different zero-concentration values because each sensor is operated at a different DC bias resulting in a different electrochemical equivalent circuitry model and thus different y-intercepts in Fig. 6. The sensitivity performance of the gas sensor array is summarized in Table V.

Only impedance mode was used for CH_4 and SO_2 measurement because they are sensed by an adsorption principle under applied DC voltages where no redox reaction occur and no faradic current is generated at the electrode/IL interface. Response time, selectivity, long term stability and reproducibility performance of PEoPM sensor responding to CH_4 were reported in[7]. Due to a novel adsorption detection principle [7], little current is consumed by the CH_4 and SO_2 sensors. Using microfabrication, the reduced electrodes sizes result in smaller volumes for all sensors and smaller redox currents for O_2 and NO_2 sensors. Comparisons of current consumption and sensor area between our sensors and several commercial sensors are given in Table VI. For a fair comparison, sensor consumed currents were all calculated at the same response points: 5% CH_4, 20.9% O_2, 20ppm SO_2 and 20ppm NO_2, and sensor volume is determined without packaging. Commercial sensor's sensing area consists of electrolytes and electrodes, as defined in datasheets; while our sensors' sensing area is defined as the cube including the O-ring, PEoPM sheet, IL and two rigid clamping boards. Our sensors have the lowest current consumption and the second smallest volume in Table VI. Although the MOS sensor has the smallest volume, it consumes significantly more current due to
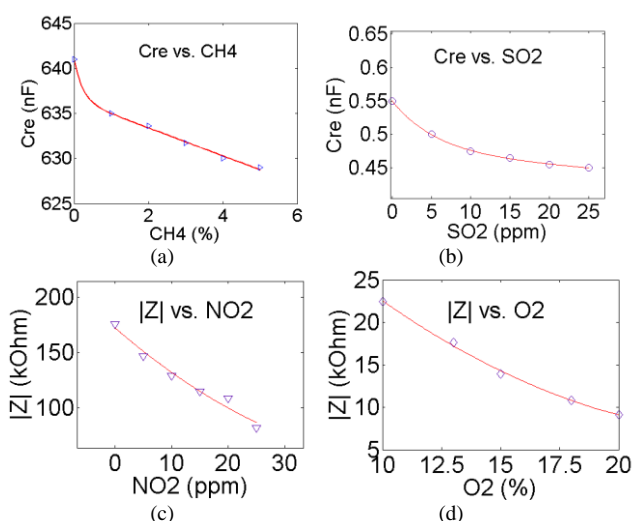

Fig. 6: Calibration curves of AC impedance response for the RTIL electrochemical gas sensor array. The discrete points were measured by a VersaSTAT4. (a) and (b) show sensor capacitance responses to CH_4 and SO_2, respectively. (c) and (d) show sensor impedance magnitudes responses to NO_2 and O_2, respectively.

Table V. Target gas ranges and sensitivities of sensor array

Gases	Concentration range	Sensitivity
CH_4	0%~5%	1.5nF/% @5%
O_2	1%~20%	0.7kohm/% @20%
SO_2	0ppm~25ppm	1.4fF/ppm @25ppm
NO_2	0ppm~25ppm	2.2kohm/ppm @25ppm

heater operation. In contrast, the largest power consumed by a sensor in our array is only 3.2μW for the O_2 sensor. In addition, our sensors uniquely support two EC measurement modes.

The MEIB instrumentation circuit was characterized in amperometry mode and EIS mode, separately. In amperometry mode, the MEIB was set at a small gain and the input current generator (Keithley 6430) was swept from -20μA to 20μA in steps of 10nA to determine the maximum current input range. As shown in Fig. 7 (a), the effective input current magnitude ranges bidirectionally from 1μA to 20μA with an output error ratio below 0.5%. Input current lower than 1μA can be achieved by selecting a larger gain. To characterize the current detection limit, the MEIB was set at the largest gain and the input current generator (Keithley 6430) was swept from -10nA to 10nA in steps of 0.01nA. Test data, regression line and output error are plotted in Fig. 7 (b). With detection limit defined as three times the regression line standard error divided by the regression line

Table VI. Comparison among gas sensors for current consumption and volume. All sensor currents were calculated for response to 5% CH_4, 20.9% O_2, 20ppm SO_2 and 20ppm NO_2, and the volumes represent sensing areas without package.

Sensors		Current consumption				Volume	Type
		CH_4	O2	SO2	NO2		
Our sensors	Amperometry mode	-	**1.9μA**	-		**350mm³**	EC
	AC impedance mode	**24.5nA**	**2.7μA**	**67.3nA**	**160.1nA**		
Commercial sensors	Alphasense / CH-D3	63.3mA	-	-	-	652 mm³	Catalytic
	Dynament / MSH-DP-HC/CO2	75~85 mA	-	-	-	2933mm³	Infrared
	Figaro / TGS 2611	56mA[a]	-	-	-	159 mm³[3c]	MOS
	SGX / EC410	-	300~400μA[b]	-	-	3857 mm³	EC
	Alphasense / O2-G2	-	30 ~42μA[b]	-	-	1261mm³	EC
	SGX / EC4-20-SO2	-	-	4 ~12μA[b]	-	3337mm³	EC
	Alphasense / SO2-BF	-	-	6~9.6μA[b]	-	1283 mm³	EC
	SGX / EC4-20-NO2	-	-	-	9 ~15μA[2]	3338mm³	EC
	Alphasense / NO2-A1	-	-	-	8 ~15μA[2]	1296mm³	EC

[a]Heater current is included in sensor current; [b] Values with ranges are taken directly from datasheets and originate from device mismatch.
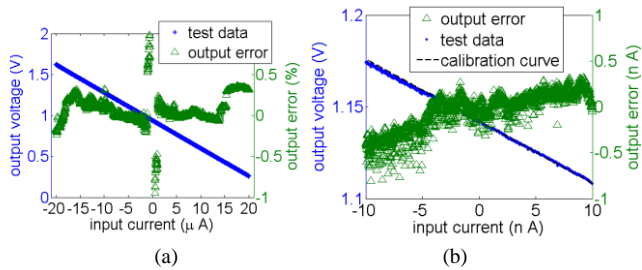
Fig. 7. Amperometric mode instrumentation output range and output errors as a function of input currents. (a) Input current was varied from -20μA to 20μA in steps of 10nA at; (b) Input current was varied from -10nA to 10nA in steps of 0.01nA.

slope, results show the current detection limit is 0.34nA. Therefore, the MEIB instrumentation can measure currents from 0.34nA to 20μA bidirectionally in amperometry mode by setting the gain to different values. The dynamic range at the largest MEIB gain setting is 29.4dB. A 5-bit ADC is sufficient to cover this dynamic range.

The MEIB instrumentation was also characterized in EIS mode. A simplified Randles cell model commonly used for EC instrumentation characterization[28-30] was adopted to construct a sensor emulation circuit. Although a more accurate model might be needed for interface characterization, this simplified model is sufficient for our instrumentation testing. Fig. 8 shows the Randles model, where R_{ct1} and R_{ct2} represent charge-transfer resistances, C_{dl1} and C_{dl2} represent double-layer capacitances, R_{s1} and R_{s2} denote solution resistances and RE, CE, WE denote electrode terminals. Based on our prior IL EC gas sensor measurements, R_{ct1} and R_{ct2} were set to 10MΩ, C_{dl1} and C_{dl2} were set to 1μF, and R_{s1} and R_{s2} were set to 10Ω. Thus, |Z| is equal to 159kohm at 1Hz, which is within the measured impedance range in Fig. 6. The EIS stimulation signal amplitude was set at 10mV and frequencies around the nominal EIS operation frequency of 1Hz were tested. Fig. 9 (bottom) plots the measured MEIB instrumentation impedance amplitude output vs. frequency. Error ratio defined as the difference between tested impedance values and the ideal impedance spectrum divided by ideal impedance, is also plotted in Fig. 9 (top) and show the MEIB circuit output matches the ideal data very well with the largest output error ratio less than 1%.

To characterize the response of the overall iEGAS system, the sensor array was connected to the custom MEIB and tested using O_2 as an example target gas. The resulting MEIB outputs in AC impedance and constant-potential amperometry mode are shown in Fig. 10 along with the corresponding calibration curves. The difference in AC impedance mode calibration curves between Fig. 10 (b) and Fig. 6 is due to the use of different sensor devices in the two tests. The long settling time when concentrations are changed is not due to O_2 sensor response time but rather to the limitations of the gas chamber that requires at least 5minutes stabilize to a new gas concentration. Response time on the order of 10 sec have been reported for the PEoPM IL gas sensor[7].System and sensor performance parameters measured from the iEGAS prototype system are summarized in Table VII, including a maximum
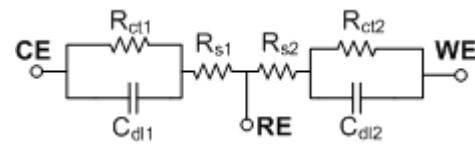

Fig. 8. Simplified Randles model equivelant circuit of EC cell. R_{ct1} and R_{ct2} represent charge-transfer resistances, C_{dl1} and C_{dl2} represent double-layer capacitances, and R_{s1} and R_{s2} denote solution resistances.
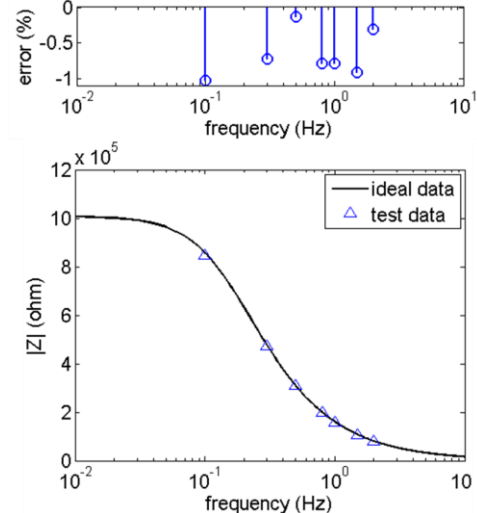

Fig. 9. EIS mode MEIB instrumentation output for a 10mV stimulation signal at frequencies of0.1Hz, 0.3Hz, 0.5Hz, 0.8Hz, 1Hz, 1.5Hz and 2Hz to cover our EC sensors 'nominal operation frequency of 1Hz. Lower plot: impedance spectrum comparison between ideal curve and test data; Upper plot: output

response resolution of 0.01vol% in amperometry mode and 0.06vol%in AC impedance mode for the example O_2target gas.

V. CONCLUSION

The development of a wearable, low-cost, low-power, multi-analytes intelligent gas sensor array system, from concept to prototype has been reported. Application-critical system performance requirements were mapped to component-level decisions within each design layer. Comparison of gas sensor techniques led to the choice of an electrochemical sensor featuring RTILs to provide low power
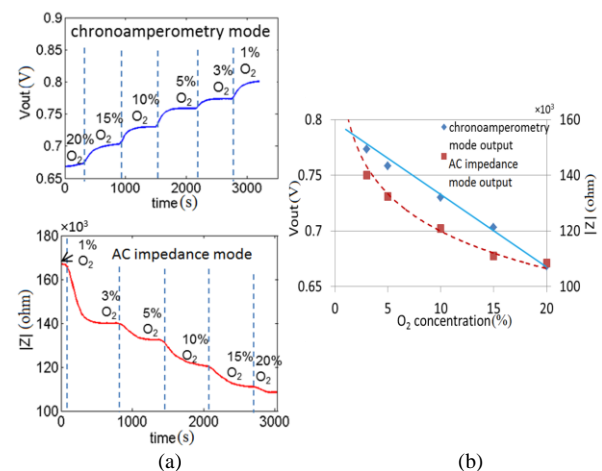

Fig. 10. (a) MEIB outputs for sensor array with O_2 concentration from 1% to 20% using (top) chronoamperometry mode and (bottom) AC impedance mode. (b) O_2 calibration curves for data in (a). The chronoamperometry O_2 response shows good linearity with an R-squared value of 0.98.

Table VII. iEGAS system performance

System	
Dimension	2.6inch×2inch×1inch
Weight	1.6 Oz
Power	6.4 mW
Detection modes	Amperometry Impedance spectroscopy
Monitored gases	CH_4 SO_2 NO_2 O_2
O_2 response: amperometry mode	Sensitivity: 6.5mV/% Resolution[1]: 0.01%
O_2 response: AC impedance mode @20% O_2	Sensitivity: 1.36kohm/% Resolution[1]: 0.06%

[1] resolution =system output noise divided by system sensitivity

consumption, small size, high sensitivity, good selectivity, and low cost. A prototype system was constructed using a plug-in custom miniaturized RTIL sensor array, a custom multi-mode electrochemical sensor instrumentation board, and a commercial low power microcontroller board. Our electrodes-on-permeable-membrane structure effectively reduces sensor response time by a factor of 100, from 98s to 8s. By utilizing the sensor's adsorption mode and miniaturizing the sensor electrodes with microfabrication processes, each sensor cell consumes less than 3.2μWandoccupiesonly28%ofa typical commercial EC gas sensor's volume. A novel resource-sharing instrumentation architecture effectively decreases power, cost and size. Regression models for the enhancement of selectivity of gas sensor array were studied in terms of their prediction accuracy and execution time on μC. Initial analysis shows the regression tree algorithm consumes the lowest power while the linear model tree algorithm achieves the least error for iEGAS-like systems. The iEGAS prototype system achieves system-level critical performance goals including high resolution gas measurements and low power consumption, demonstrating that it is a suitable platform for further miniaturization toward a wearable multi-gas monitoring system for human safety and health and a valuable new tool for the assessment of personal exposure to environmental and occupational hazards.

ACKNOWLEDGMENT

REFERENCES

[1] R. Brook, "Cardiovascular effects of air pollution," *Clinical Science,* vol. 115, pp. 175-187, 2008.

[2] J. W. Gardner, *et al.*, "CMOS interfacing for integrated gas sensors: A review," *Sensors Journal, IEEE,* vol. 10, pp. 1833-1848.

[3] P. Zhang, *et al.*, "Design of wireless mine gas monitoring and control system based on nRF2401," in *Computer Science & Service System (CSSS), 2012 International Conference on*, 2012, pp. 1051-1054.

[4] F. Tsow, *et al.*, "A wearable and wireless sensor system for real-time monitoring of toxic environmental volatile organic compounds," *Sensors Journal, IEEE,* vol. 9, pp. 1734-1740, 2009.

[5] K.-T. Tang, *et al.*, "A 0.5 V 1.27 mW nose-on-a-chip for rapid diagnosis of ventilator-associated pneumonia," in *Solid-State Circuits Conference Digest of Technical Papers (ISSCC), 2014 IEEE International*, 2014, pp. 420-421.

[6] K. T. Ng, *et al.*, "A CMOS single-chip gas recognition circuit for metal oxide gas sensor arrays," *Circuits and Systems I: Regular Papers, IEEE Transactions on,* vol. 58, pp. 1569-1580, 2011.

[7] Z. Wang, *et al.*, "Methane recognition and quantification by differential capacitance at the hydrophobic ionic liquid-electrified metal electrode interface," *Journal of the Electrochemical Society,* vol. 160, pp. 83-89, 2013.

[8] X. Mu, *et al.*, "A robust flexible electrochemical gas sensor using room temperature ionic liquid," *Sensors Journal, IEEE,* vol. 13, pp. 3976 - 3981, 2013.

[9] Z. Wang, *et al.*, "Ionic liquids as electrolytes for the development of a robust amperometric oxygen sensor," *Analytical Chemistry,* vol. 83, pp. 7066-7073, 2011.

[10] H. Li, *et al.*, "Room temperature ionic-liquid electrochemical gas sensor array system for real-time mine safety monitoring," in *IEEE International Conference on Sensors*, Baltimore, 2013, pp. 1-4.

[11] H. Kramer and K. Mangieri, "Review of sensor technologies used in portable gas monitors," Industrial Scientific Corporation.

[12] R. Knake, *et al.*, "Amperometric detection of gaseous formaldehyde in the ppb range," *Electroanalysis,* vol. 13, pp. 631-634, 2001.

[13] G. Schiavon, *et al.*, "Amperometric monitoring of ozone in gaseous media by gold electrodes supported on ion exchange membranes (solid polymer electrolytes)," *Analytical Chemistry,* vol. 62, pp. 293-298, 1990.

[14] A. W. E. Hodgson, *et al.*, "Electrochemical sensor for the detection of SO2 in the low-ppb range," *Analytical Chemistry,* vol. 71, pp. 2831-2837, 1999.

[15] S. S. Bhoga and K. Singh, "Electrochemical solid state gas sensors: An overview," *Ionics,* vol. 13, pp. 417-427, 2007.

[16] P. Jasiński, "Solid-state electrochemical gas sensors," *Materials Science-Poland,* vol. 24, pp. 269-278, 2006.

[17] M. C. Buzzeo, *et al.*, "Kinetic analysis of the reaction between electrogenerated superoxide and carbon dioxide in the room temperature ionic liquids 1-ethyl-3-methylimidazolium bis (trifluoromethylsulfonyl) imide and hexyltriethylammonium bis (trifluoromethylsulfonyl) imide," *The Journal of Physical Chemistry B,* vol. 108, pp. 3947-3954, 2004.

[18] R. Wang, *et al.*, "A novel amperometric O2 gas sensor based on supported room-temperature ionic liquid porous polyethylene membrane-coated electrodes," *Electroanalysis,* vol. 16, pp. 66-72, 2004.

[19] X. Huang, *et al.*, "Toward membrane-free amperometric gas sensors: A microelectrode array approach," *Analytical Chemistry,* vol. 82, pp. 5238-5245, 2010.

[20] M. A. G. Zevenbergen, *et al.*, "Electrochemical sensing of ethylene employing a thin ionic-liquid layer," *Analytical Chemistry,* vol. 83, pp. 6300-6307, 2011.

[21] "Electrochemical sensors application note 2: Design of electronics for electrochemical gas sensors," SGX Sensortech (IS) Ltd.2010.

[22] L. Carmel, *et al.*, "On predicting responses to mixtures in quartz microbalance sensors," *Sensors and Actuators B: Chemical,* vol. 106, pp. 128-135, 2005.

[23] K.-T. Tang, *et al.*, "A low-power electronic nose signal-processing chip for a portable artificial olfaction system," *Biomedical Circuits and Systems, IEEE Transactions on,* vol. 5, pp. 380-390, 2011.

[24] Y. Yang, *et al.*, "Power-error analysis of sensor array regression algorithms for gas mixture quantification in low-power microsystems," in *IEEE International Conference on Sensors*, Baltimore, 2013.

[25] A. Ziyatdinov, *et al.*, "Drift compensation of gas sensor array data by common principal component analysis," *Sensors and Actuators B: Chemical,* vol. 146, pp. 460-465, 2010.

[26] X. Mu, *et al.*, "Fabrication of a miniaturized room temperature ionic liquid gas sensor for human health and safety monitoring," in *Biomedical Circuits and Systems Conference (BioCAS), 2012 IEEE*, 2012, pp. 140-143.

[27] M. E. Orazem and B. Tribollet, *Electrochemical impedance spectroscopy* vol. 48: John Wiley & Sons, 2011.

[28] M. M. Ahmadi and G. A. Jullien, "Current-mirror-based potentiostats for three-electrode amperometric electrochemical sensors," *Circuits and Systems I: Regular Papers, IEEE Transactions on,* vol. 56, pp. 1339-1348, 2009.

[29] S. Sutula, *et al.*, "A 25-μW All-MOS Potentiostatic Delta-Sigma ADC for Smart Electrochemical Sensors," *Circuits and Systems I: Regular Papers, IEEE Transactions on,* vol. 61, pp. 671 - 679, 2014.

[30] M. H. Nazari, *et al.*, "CMOS neurotransmitter microarray: 96-channel integrated potentiostat with on-die microsensors," *Biomedical Circuits and Systems, IEEE Transactions on,* vol. 7, pp. 338-348, 2013.